

Quench of the electronic order in a strongly-coupled charge-density-wave system by enhanced lattice fluctuations

Manuel Tuniz,^{1,2,*} Denny Puntel,¹ Wibke Bronsch,³ Francesco Sammartino,¹ Gian Marco Pierantozzi,² Riccardo Cucini,² Fulvio Parmigiani,^{1,3,4} and Federico Cilento^{3,†}

¹*Dipartimento di Fisica, Università degli Studi di Trieste, 34127 Trieste, Italy*

²*CNR - Istituto Officina dei Materiali (IOM), Unità di Trieste, Strada Statale 14, km 163.5, 34149 Basovizza (TS), Italy*

³*Elettra - Sincrotrone Trieste S.C.p.A., Strada Statale 14, km 163.5, Trieste, Italy*

⁴*International Faculty, University of Cologne, Albertus-Magnus-Platz, 50923 Cologne, Germany*

(Dated: March 7, 2025)

Charge-density-wave (CDW) materials having a strong electron-phonon coupling provide a powerful platform for investigating the intricate interplay between lattice fluctuations and a macroscopic quantum order. Using time- and angle-resolved photoemission spectroscopy (TR-ARPES), we reveal that the CDW gap closure in VTe₂ is dominated by an incoherent process evolving on a sub-picosecond timescale, challenging the conventional view that the gap dynamics is primarily governed by the excitation of the CDW amplitude modes. Our findings, supported by a three-temperature model, show that the CDW gap evolution can be described by considering the population of a subset of strongly-coupled optical phonon modes, which leads to an increase in the lattice fluctuations. This microscopic framework extends beyond VTe₂, offering a universal perspective for understanding the light-induced phase transition in strongly-coupled CDW systems.

I. INTRODUCTION

Among the various microscopic interactions shaping quantum materials, electron-phonon coupling (EPC) has been a persistent subject of study since it stands at the origin of a broad variety of phenomena. One of the manifestations of strong EPC, which is lately attracting a large interest, is the appearance of a charge-density wave (CDW) phase in many materials [1–3]. In CDW systems, electrons and phonons cooperatively interact to form a new symmetry-broken state below a critical transition temperature [4]. The resulting low-temperature phase is characterized by the coexistence of a spatial modulation of the electron density and a periodic distortion of the crystalline structure [4]. While the charge-density-wave transition has been traditionally described in the weak EPC limit [5], the discovery of compounds exhibiting strong momentum-dependent EPC has motivated both theoretical [6–9] and experimental studies [10–12]. Due to the complexity of these systems, however, a unified microscopic understanding of the CDW transition and its dynamics remains elusive [1].

Giving the pivotal role played by the EPC in determining the CDW phase transition, an increase of its strength leads to a dramatic deviation from the conventional Peierls picture of the CDW transition [4, 13]. Indeed, while in the weak-coupling limit the transition from the CDW to the normal phase is driven by the electronic entropy, in the strong-coupling limit the phase transition is instead driven by the lattice entropy, thus resulting in an order-disorder transition [6, 14]. As a result, strongly-

coupled CDW materials provide a compelling platform to study the interplay between lattice fluctuations and the emergence of a macroscopic quantum order. Furthermore, controlling the CDW phase and understanding its ultrafast dynamics are essential steps toward the development of next-generation electronic devices based on these materials [15]. More broadly, lattice fluctuations are not only key to understand the CDW dynamics in VTe₂, but they are also believed to play a crucial role in the phase transition of a wide range of quantum materials [16, 17].

In this work, studying the CDW gap dynamics by means of TR-ARPES experiments, we demonstrate that in the strongly-coupled CDW compound VTe₂, the light-induced phase transition is determined by an incoherent process that evolves on a timescale much slower than the one expected for a conventional displacive transition [17]. By implementing a three-temperature model, we demonstrate that the CDW gap dynamics can be described considering the population of a subset of strongly-coupled optical phonon modes, which determine an increase of the lattice fluctuations, and hence of the transient disorder of the system.

II. METHODS

High-quality VTe₂ single crystals were provided by HQ Graphene. The samples were cleaved *in situ*, at a base pressure better than 5×10^{-10} mbar and at room temperature. ARPES and TR-ARPES experiments were performed using a state-of-the-art HHG source equipped with a time-preserving monochromator and synchronized to an OPA system delivering the pump pulses [18]. For the present experiments, the pump and probe photon energies were set to 1.77 and 21.6 eV respectively. The ultimate energy and time resolutions were ~ 55 meV and

* manuel.tuniz@phd.units.it

† federico.cilento@elettra.eu

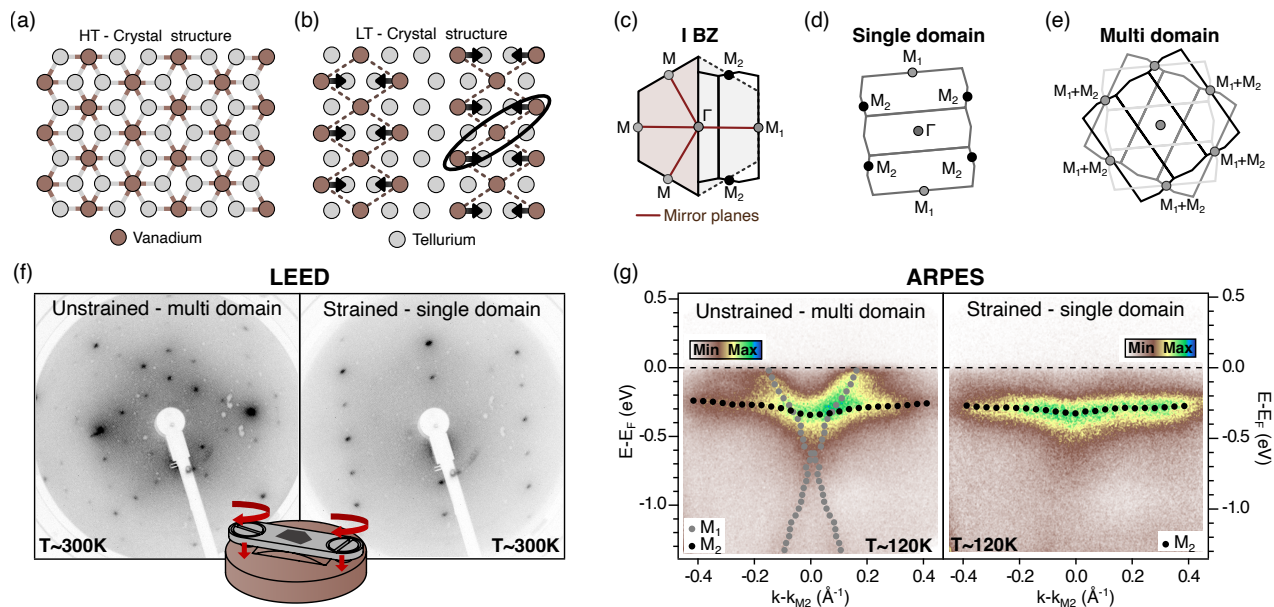


FIG. 1. (a) Projection of a high-temperature (HT) single VTe_2 layer on the pseudo-hexagonal plane. (b) Projection of a low-temperature (LT) single VTe_2 layer on the pseudo-hexagonal plane. The black arrows show the displacement direction of the vanadium atoms, while the black ellipse and dashed lines highlight the formation of a trimer-like bonding between three vanadium atoms, resulting in a double zigzag structure. (c) High-temperature (left) and low-temperature (right) first Brillouin zones of VTe_2 . The mirror planes of the two BZs are also shown. (d) View of the reciprocal space as seen by a probe beam smaller than the size of the domains. (e) View of the reciprocal space as seen by a probe beam larger than the domain size. Due to the averaging over different domains, the M_1 and M_2 points are perfectly overlapped. (f) LEED images taken before (left panel) and after (right panel) the application of strain on the same VTe_2 sample. A single domain with 3×1 superstructure is observed in the strained case. The images have been taken with a kinetic energy of 75 eV. The inset depicts the strain device used in the experiments. (g) ARPES spectra acquired along the K - M_2 - K direction on an unstrained (left) and on a strained (right) samples.

~ 110 fs, respectively, while the FWHM of the probe beam at the sample position was of the order of $100 \mu\text{m}$. An home-built strain device was mounted on the sample holder, to perform photoemission experiments on strained samples (further details are reported in the SM).

III. EXPERIMENTAL RESULTS

Strain-induced domain stabilization

In the transition-metal dichalcogenide compound VTe_2 , the presence of a strong EPC results in the opening of a CDW gap whose size is five times larger than the one predicted by the weak-coupling limit, making this compound an ideal candidate for studying the effect of enhanced lattice fluctuations on the CDW phase [4]. However, the study of the gap dynamics is hindered by the presence of multiple CDW domains that characterize the low-temperature phase. Indeed, at 480 K the system undergoes a first order phase transition towards a new commensurate $3 \times 1 \times 3$ charge-ordered phase (Fig. 1(a) and (b)), that leads to the formation of three equivalent in-plane domains, rotated by 120 degrees [19–21]. As depicted in Fig. 1(d) and (e), when a probe beam larger than the typical domain size is used, the resulting super-

position of BZs causes the M_1 and M_2 points to overlap, thereby hindering the study of the CDW gap that opens at the M_2 point. To overcome this issue, following an emerging approach to control the domain structure of complex materials [22], we developed a strain device capable of delivering uniaxial tensile strain to the VTe_2 crystals. By breaking the equivalence between the different domains, the application of strain results in the formation of larger domains. The effectiveness of this approach was assessed by means of low energy electron diffraction (LEED) and ARPES experiments. Figure 1(f) shows a comparison between two LEED images acquired on the same sample before (left) and after (right) the application of a tensile strain of $\sim 0.2\%$ (details on the strain application and its quantification are reported in the SM). The effect of the applied strain is clearly visible from these images. While the complex pattern that appears in the unstrained sample arises from the superposition of the three different domains, the one observed on the strained sample clearly denotes the presence of a single domain in the probed region. To further confirm the effectiveness of our approach, in Fig. 1(g) we report a comparison between two ARPES spectra acquired on an unstrained (left) and on a strained (right) samples. As for the LEED image, the ARPES map acquired on the unstrained sample shows a superposition of bands com-

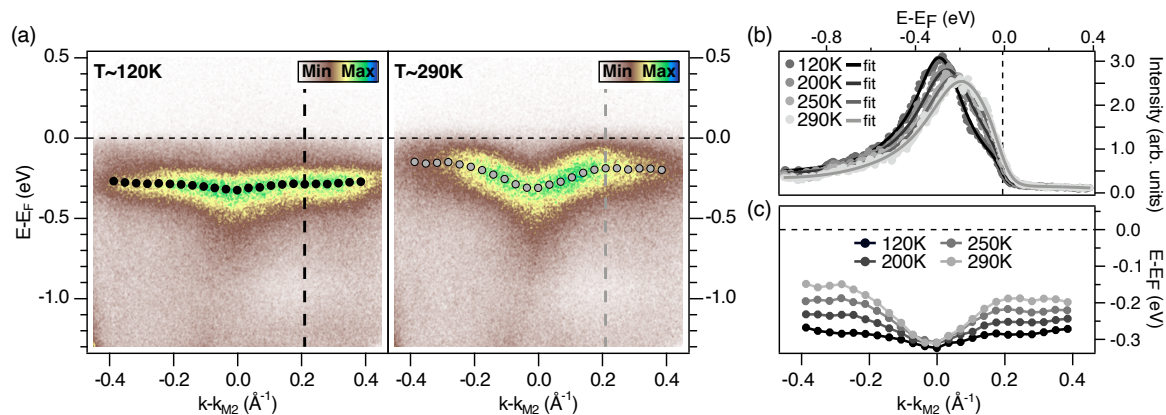


FIG. 2. (a) Photoemission spectra acquired along the K-M₂-K direction at 120 K and 290 K. The grey circles denote the central position of the Lorentzian peaks used to fit the EDCs, hence they show the dispersion of the vanadium 3d band. (b) EDCs extracted from the momentum region denoted by the dashed lines in (a) for four temperatures. (c) Evolution of the dispersion of the hybridized vanadium 3d band as a function of the temperature.

ing from the M₁ and the M₂ points of different Brillouin zones (BZs) [23]. In contrast, the ARPES map acquired on the strained sample only shows the nearly-flat band from the M₂ point. These spectra therefore demonstrate the possibility of performing photoemission experiments on a single domain by applying a tensile strain to the VTe₂ crystals. Since the only detectable effect of the applied strain is the promotion of larger domains, all the ARPES experiments presented below were performed on strained samples.

ARPES measurements

We start by analyzing the effect of a temperature change on the CDW gap that opens at M₂. Figure 2(a) shows the band structure measured along the K-M₂-K direction, at 120 and 290 K. As shown in Fig. 1(c), in the normal phase, the M points reside on a mirror plane which prohibits the hybridization between the Te 5p orbitals (odd with respect to the mirror plane) and the V 3d orbitals (even with respect to the mirror plane). In the low temperature phase, instead, while the M₁ points keep a similar situation with respect to the high-temperature phase, the M₂ points do not reside anymore on a mirror plane. Hence the V 3d and the Te 5p orbitals can now mix, leading to a significant change in the band structure [23]. The V-shaped band that characterizes the M points in the normal phase of VTe₂ is replaced by a weakly-dispersing band at $E_B \sim 0.25$ eV, whose flatness reflects the localized nature of the d_{yz} and d_{zx} orbitals in real space [23]. As expected from the change in the lattice symmetry, by increasing the temperature, we observe a folding of the hybridized vanadium 3d band towards the Fermi level, in such a way that the V-shaped band is partially restored. Figures 2(b) and (c) show the evolution of the position of the vanadium band (details on the fitting procedure are reported in the SM) as a function of

temperature. Despite the presence of a first order phase transition, far from the critical temperature we observe a progressive folding of the vanadium band, with the consequent partial closure of the CDW gap.

TR-ARPES measurements

Having characterized the temperature-driven phase transition, we now investigate the possibility to melt the CDW order using an ultrashort pump pulse ($h\nu_{\text{pump}} = 1.77$ eV). Figure 3 shows three ARPES spectra acquired at different pump-probe delays, along with the differential maps that highlight the changes induced by the pump pulse. Panels (a)-(c) show that, after photoexcitation, the dispersion of the vanadium band is modified in a way similar to the one observed in the temperature-driven phase transition. In particular, we observe a partial reappearance of the V-shaped band that characterizes the normal phase of VTe₂. Interestingly, from the comparison of the three spectra it appears that the changes in the dispersion of the vanadium 3d band are more pronounced in the spectrum acquired at a pump-probe delay of 500 fs than in the one at 100 fs. These differences are well resolved in the differential images shown in Fig. 3(e) and (f), where two qualitatively different scenarios appear. While at 100 fs (panel (e)) only the fingerprint of a small shift of the whole vanadium band towards the Fermi level is detected, the pattern visible in panel (f) is likely to arise from the folding of the vanadium band. To study the full dynamics of the vanadium band, in Fig. 3(g) and (h) we report the evolution of the EDCs and the differential EDCs (dEDCs), integrated in the momentum region delimited by the dashed lines shown in Fig. 3(c) and (f), as a function of the pump-probe delay. Having verified that the dynamics extracted from the two sides (left and right with respect to $k-k_{M_2} = 0$) of the vanadium band are equivalent, here only the ones extracted

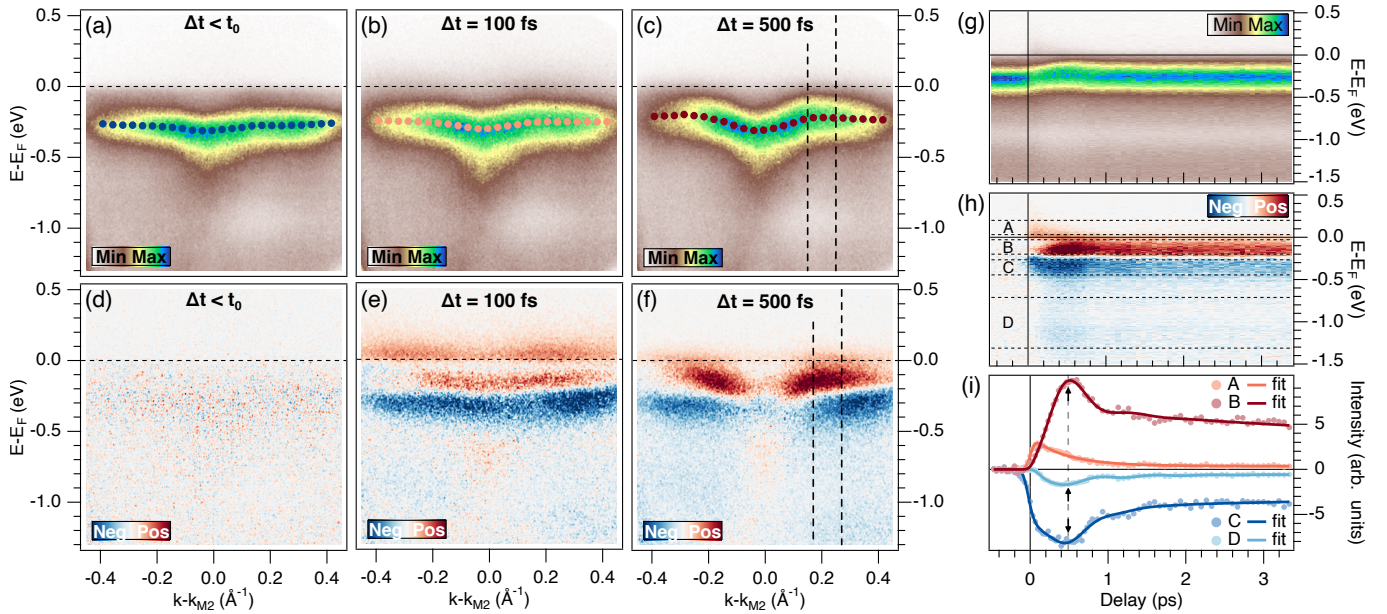


FIG. 3. (a)-(c) Selected ARPES spectra acquired along the K-M₂-K direction at different pump-probe delays: (a) before the arrival of the pump, (b) and (c) respectively 100 and 500 fs after the arrival of the pump pulse. The colored circles denote the central position of the vanadium band extracted from the fits of the EDCs. (d)-(f) Differential ARPES maps showing the changes in the photoemission intensity induced by the pump pulse. (g) and (h) EDCs and dEDCSs extracted by integrating the photoemission intensity from the momentum region delimited by the dashed lines in (c) and (f), plotted as a function of the pump-probe delay. (i) Evolution of the photoemission intensity extracted from the boxes reported in (h). The gray dashed line shows the pump-probe delay at which traces B and C reach their maximum change. The measurements were performed at a base temperature of ~ 120 K, and using an absorbed fluence of ~ 1.2 mJ/cm².

from the right side of the V-shaped band are analyzed. Figure 3(i) shows the traces obtained by integrating the photoemission intensity inside the boxes drawn in panel (h). While trace A shows a rise time limited only by the time resolution of the setup, and reaches its maximum about ~ 100 fs after the arrival of the pump pulse, the other traces show larger rise times. In particular, the maximum change for traces B and C is recorded at a pump-probe delay of ~ 500 fs, indicating that the folding of the vanadium band, and the consequent closure of the CDW gap, evolves on a much slower timescale with respect to the one of the hot carriers described by trace A. Moreover, the absence of marked oscillations in the gap size signals that the photoinduced phase transition in VTe₂ is not driven by the excitation of the CDW amplitude modes, as instead observed in many other CDW systems. Indeed, in those systems, the maximum closure of the CDW gap occurs on a timescale corresponding to half period of the CDW amplitude mode [24–29]. As demonstrated by Tuniz *et al.* [30], VTe₂ has two amplitude modes with a low-temperature frequency of 1.6 THz and 2.5 THz, for which a characteristic timescale of 300 and 200 fs would be expected, respectively. The fact that the timescales observed here are almost two times longer, suggests that the melting of the charge-ordered is not dominated by a conventional displacive process.

In general, a solid-solid phase transition, where the symmetry of the crystal is raised, can be determined by

either a displacive process or an order-disorder process [17, 31, 32]. While in a displacive transition the atoms collaboratively reshuffle their positions under the effect of a few well-defined spatially coherent vibrational modes, in an order-disorder transition the atoms move from the low to the high-symmetry structure in such a way that the motion remains correlated only along one direction, while along the others it proceeds in a spatially incoherent manner, with no characteristic correlation length [17, 33–37]. In the present case of VTe₂, the emerging picture is that the gap dynamics is determined by a loss of the long-range CDW order triggered by an increase of lattice fluctuations. We emphasize that, in the present case, the role played by the increased lattice fluctuations can be isolated only thanks to the large energy gaps that characterize the strongly-coupled CDW systems like VTe₂, which make the electronic entropy (that otherwise would have overshadowed these effects) unimportant in determining the phase transition [6].

In the light-induced process considered, the increase in the lattice fluctuations occurs as a consequence of the energy transfer from the excited electrons to the lattice [38–40]. Therefore, to model this energy flow, we implement a three-temperature model (3TM) and we compare the results obtained to the ones derived from a line shape analysis of the CDW gap (details on the fitting procedure are reported in the SM) [41]. Specifically, by fitting the dynamics of the electronic temperature ex-

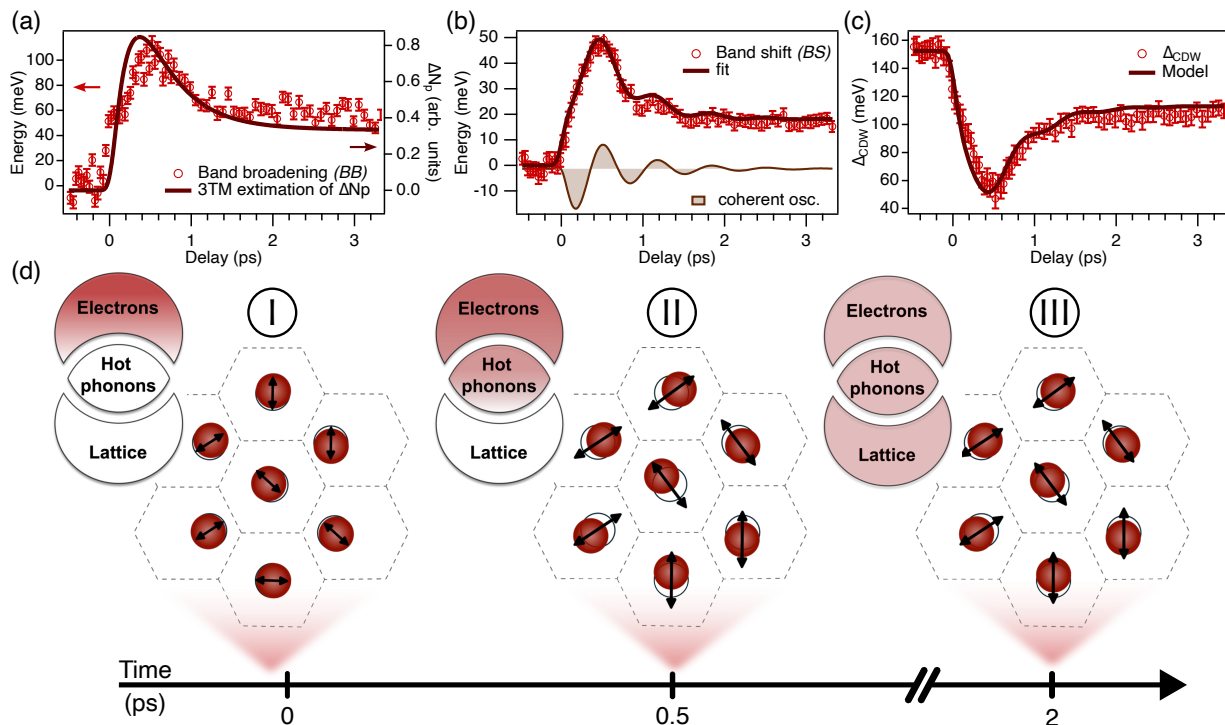


FIG. 4. (a) Comparison between the transient broadening of the CDW gap and the change in the population of the strongly-coupled optical phonon modes. (b) Fit of the CDW gap closure obtained by summing to the trace describing the transient change in the population of the strongly-coupled modes (rescaled by a constant) an oscillating term with the frequency of the CDW amplitude mode having the lowest energy. (c) Comparison between the dynamics of the CDW gap (distance between the leading edge of the lower branch and the Fermi level) and the model obtained by summing the curves shown in (a) and (b). (d) Sketch showing the partial loss of the long-range CDW order, occurring as a consequence of the incoherent excitation of the strongly-coupled optical phonon modes. The red spheres represent the vanadium atoms while the black arrows depict the amplitude of their displacements. (I) Before the arrival of the pump pulse the three subsystems are in equilibrium ($T_e = T_p = T_e \ll T_{\text{CDW}}$) and the system is characterized by a well-defined CDW order. The energy injected by the pump in the system is initially absorbed by the electrons and then transferred to a subset of strongly-coupled optical phonon modes. (II) The excitation of these phonon modes, without a macroscopic phase coherence, leads to a partial loss of the CDW long-range order of the system. (III) After ≈ 2 ps from the arrival of the pump pulse, the three subsystems are again in equilibrium and from there on the relaxation dynamics is governed solely by heat diffusion.

tracted at M_1 , we can derive the temperature evolution of the optical phonon modes which are more strongly coupled to the electronic system. These simulations were performed assuming the phonon branch at $\omega_p \sim 24$ meV to be the one more strongly coupled, with a resulting e-ph coupling constant of $\lambda = 0.32$ (a detailed discussion is reported in the SM). Starting from the evolution of the temperature (T_p) of these strongly-coupled modes, and assuming that their population (n_p) can be described by the Bose-Einstein distribution:

$$n_p(t) \propto \left[\exp\left(\frac{\hbar\omega_p}{k_B T_p(t)}\right) - 1 \right]^{-1}, \quad (1)$$

it is possible to calculate the change in the population of the strongly-coupled modes due to the increase of their temperature, triggered by the hot carrier relaxation [39]. We emphasize that these modes are excited without a macroscopic phase coherence, and therefore their excitation leads to an increase of the lattice fluctuations in the system. Increased lattice fluctuations give rise to a

smearing of the gap edges [42, 43], therefore establishing a link between the transient disorder in the system and the broadening of the CDW gap [44].

We proceed by comparing the timescales over which these processes evolve. Figure 4(a) shows a comparison between the transient broadening ($BB(t)$) of the CDW gap and the change in the population of the strongly-coupled modes ($\Delta n_p(t)$). Interestingly, these two traces evolve on similar timescales. The excitation of the strongly-coupled optical phonon modes is governed by the hot carrier relaxation through the electron-phonon coupling constant, therefore the maximum change in the population of the modes is achieved only 400 – 500 fs after the arrival of the pump pulse. This timescale matches well the one observed for the smearing of the CDW gap. Moreover, also the second relaxation process of both traces is similar, with the two showing a slow recovery dynamics for pump-probe delays larger than 2 ps.

The results obtained by applying the 3TM can be used to model also the dynamics of the gap closure. Indeed,

the broadening of the gap discussed above entails a reduction of the gap size itself, and therefore a reduction of the energy gain of the electronic subsystem with the consequent reduction of the amplitude of the lattice distortion. With this in mind we can compare the incoherent dynamics of the closure of the CDW gap with the one describing the change in the population of the strongly coupled optical phonon modes (rescaled by a constant factor). Moreover, given the presence of small bumps in the trace showing the evolution of the band shift, on top of this incoherent dynamics we summed a damped cosine oscillation with the frequency of the lowest-energy CDW amplitude mode [30]. Therefore, the evolution of the band shift (BS) has been modeled using the equation:

$$BS(t) = A \cdot \Delta n_p(t) + I e^{-t/\tau} \cos(\omega_{AM}t + \phi), \quad (2)$$

where A is the constant used to rescale the change in the population of the strongly-coupled modes. I is the intensity of the oscillating component with angular frequency ω_{AM} , decay time τ and phase ϕ . The result of the fit obtained by using Eq. 2 is shown in Fig. 4(b), together with the coherent part of the fit, reported separately. As for the case of the gap broadening, the timescales extracted from the 3TM match well with the ones extracted from the experiments, hence corroborating the thermal origin of the dynamics observed.

Finally, being able to describe the dynamics of both gap closure and gap broadening in terms of the change in the population of the strongly-coupled modes, it is possible to sum together the two models to describe the dynamics of the CDW gap:

$$\Delta_{CDW}(t) = \Delta_{CDW}(0) - BS(t) - \frac{1}{2}BB(t), \quad (3)$$

which has been obtained using the edge-midpoint definition [45–47] (see the SM for further details). The comparison between the gap dynamics and our model is reported in Fig. 4(c).

IV. DISCUSSION

We can now summarize the microscopic physical picture that stands at the base of the comparison between the dynamics obtained from the 3TM and the ones extracted from the fits of the EDCs (Fig. 4(d)). Before the arrival of the pump pulse, the three subsystems given by electrons, hot phonons and lattice are in equilibrium, and their temperature is much lower than the CDW critical temperature: $T_e = T_p = T_l \ll T_{CDW}$. Hence, the compound is characterized by a well-defined long-range CDW order. After the arrival of the visible pump pulse, the energy injected in the system is absorbed by the electrons and then transferred to the subset of strongly-coupled optical phonon modes (as expected from this picture, the dynamics does not depend on the pump photon energy, see the SM). The crucial point is that the excitation of

these modes occurs without a macroscopic phase coherence, thus leading to a partial loss of the long-range order of the system [17]. This partial loss of the long-range order, that evolves on the same timescale of the population of the strongly-coupled phonon modes, entails a smearing and a partial closure of the CDW gap. Furthermore, additional simulations (reported in the SM) show that the dynamics of the CDW gap remains well described if any phonon energy between 19 and 38 meV is considered. This result suggests a scenario in which not just a single phonon branch, but instead different branches, enclosed in a specific energy region, are involved in the disordering of the vanadium trimers, similarly to what was observed for the case of VO_2 [17, 31, 48–50]. After a first thermalization, electrons and hot phonons reach a common temperature and their dynamics become similar. Subsequently, the relaxation proceeds via anharmonic phonon-phonon interaction, which continues until a thermal equilibrium with all the other modes is reached. From here on, the relaxation is governed only by thermal diffusion, and hence it evolves on a much slower timescale, not captured by the 3TM. Therefore, this microscopic picture also explains the dynamics observed at large pump-probe delays, *i.e.* the presence of a plateau in both the gap closure and the gap broadening. At these delays the strongly coupled phonon modes have reached a common temperature with all the other modes, hence the relaxation process is brought forward on a much slower timescale solely by heat diffusion [51].

V. CONCLUSIONS

In conclusion, we showed that the light-induced phase transition in VTe_2 can be fully described by considering the population of a subset of strongly-coupled optical phonon modes, with only a marginal role played by the excitation of the CDW amplitude modes. The excitation of the strongly-coupled phonons, which occurs without a macroscopic phase coherence, has the effect of increasing the lattice fluctuations and thus the transient disorder of the system [25, 39]. The microscopic picture developed extends beyond the specific case of VTe_2 and could be applied to other CDW systems. More generally, the results presented in this article highlight the need for a deeper understanding of the interplay between lattice fluctuations and the CDW phase, paving the way for further exploration of the nonequilibrium properties of strongly-coupled CDW systems.

VI. ACKNOWLEDGMENTS

M.T. acknowledges financial support under the National Recovery and Resilience Plan (NRRP), Mission 4, Component 2, Investment 1.1, Call for tender No. 104 published on 2.2.2022 by the Italian MUR, funded by the European Union – NextGenerationEU – Project

MEGS-CUP B53D23003930006. R.C acknowledges the Italian Ministry of Foreign Affairs and International Cooperation (MAECI), Grant no. PGR12320 - U-DYNAMEC - CUP B53C23006060001. This work is per-

formed in the framework of the Nanoscience Foundry and Fine Analysis (NFFA-MUR Italy Progetti Internazionali) facility.

-
- [1] K. Rossnagel, On the origin of charge-density waves in select layered transition-metal dichalcogenides, *Journal of Physics: Condensed Matter* **23**, 213001 (2011).
- [2] M. Kang, S. Fang, J.-K. Kim, B. R. Ortiz, S. H. Ryu, J. Kim, J. Yoo, G. Sangiovanni, D. Di Sante, B.-G. Park, C. Jozwiak, A. Bostwick, E. Rotenberg, E. Kaxiras, S. D. Wilson, J.-H. Park, and R. Comin, Twofold van Hove singularity and origin of charge order in topological kagome superconductor CsV_3Sb_5 , *Nature Physics* **18**, 301 (2022).
- [3] R. Comin, A. Frano, M. M. Yee, Y. Yoshida, H. Eisaki, E. Schierle, E. Weschke, R. Sutarto, F. He, A. Soumyanarayanan, Y. He, M. L. Tacon, I. S. Elfimov, J. E. Hoffman, G. A. Sawatzky, B. Keimer, and A. Damascelli, Charge Order Driven by Fermi-Arc Instability in $\text{Bi}_2\text{Sr}_{2-x}\text{La}_x\text{CuO}_{6+\delta}$, *Science* **343**, 390 (2014).
- [4] G. Grüner, *Density Waves In Solids* (Addison-Wesley).
- [5] G. Grüner, The dynamics of charge-density waves, *Rev. Mod. Phys.* **60**, 1129 (1988).
- [6] W. L. McMillan, Microscopic model of charge-density waves in $2H - \text{TaSe}_2$, *Phys. Rev. B* **16**, 643 (1977).
- [7] C. M. Varma and A. L. Simons, Strong-coupling theory of charge-density-wave transitions, *Phys. Rev. Lett.* **51**, 138 (1983).
- [8] J. Inglesfield, Bonding and charge density wave phase transitions, *Physica B+C* **99**, 238 (1980).
- [9] X. Zhu, Y. Cao, J. Zhang, E. W. Plummer, and J. Guo, Classification of charge density waves based on their nature, *Proceedings of the National Academy of Sciences* **112**, 2367 (2015).
- [10] R. Tediosi, F. Carbone, A. B. Kuzmenko, J. Teyssier, D. van der Marel, and J. A. Mydosh, Evidence for strongly coupled charge-density-wave ordering in three-dimensional $R_5\text{Ir}_4\text{Si}_{10}$ compounds from optical measurements, *Phys. Rev. B* **80**, 035107 (2009).
- [11] P. Hofmann, M. M. Ugeda, A. Tamtögl, A. Ruckhofer, W. E. Ernst, G. Benedek, A. J. Martínez-Galera, A. Stróżecka, J. M. Gómez-Rodríguez, E. Rienks, M. F. Jensen, J. I. Pascual, and J. W. Wells, Strong-coupling charge density wave in a one-dimensional topological metal, *Phys. Rev. B* **99**, 035438 (2019).
- [12] S. Cao, C. Xu, H. Fukui, T. Manjo, Y. Dong, M. Shi, Y. Liu, C. Cao, and Y. Song, Competing charge-density wave instabilities in the kagome metal ScV_6Sn_6 , *Nature Communications* **14**, 7671 (2023).
- [13] R. Peierls, *Quantum Theory of Solids*, International series of monographs on physics (Clarendon Press, 1955).
- [14] E. Tosatti, Surface states, surface metal-insulator, and surface insulator-metal transitions (1995), arXiv:cond-mat/9505057 [cond-mat].
- [15] I. Vaskivskiy, J. Gospodaric, S. Brazovskii, D. Svetin, P. Sutar, E. Goreschnik, I. A. Mihailovic, T. Mertelj, and D. Mihailovic, Controlling the metal-to-insulator relaxation of the metastable hidden quantum state in $1t\text{-tas}_2$, *Science Advances* **1**, e1500168 (2015).
- [16] M. Fechner, M. Först, G. Orenstein, V. Krapivin, A. S. Disa, M. Buzzi, A. von Hoegen, G. de la Pena, Q. L. Nguyen, R. Mankowsky, M. Sander, H. Lemke, Y. Deng, M. Trigo, and A. Cavalleri, Quenched lattice fluctuations in optically driven SrTiO_3 , *Nature Materials* **23**, 363 (2024).
- [17] S. Wall, S. Yang, L. Vidas, M. Chollet, J. M. Glowina, M. Kozina, T. Katayama, T. Henighan, M. Jiang, T. A. Miller, D. A. Reis, L. A. Boatner, O. Delaire, and M. Trigo, Ultrafast disordering of vanadium dimers in photoexcited VO_2 , *Science* **362**, 572 (2018).
- [18] R. Cucini, T. Pincelli, G. Panaccione, D. Kopic, F. Frassetto, P. Miotti, G. M. Pierantozzi, S. Peli, A. Fondacaro, A. De Luisa, A. De Vita, P. Carrara, D. Krizmancic, D. T. Payne, F. Salvador, A. Sterzi, L. Poletto, F. Parmigiani, G. Rossi, and F. Cilento, Coherent narrowband light source for ultrafast photoelectron spectroscopy in the 17–31 eV photon energy range, *Structural Dynamics* **7**, 014303 (2020).
- [19] K. Bronsema, G. Bus, and G. Wieggers, The crystal structure of vanadium ditelluride, $\text{V}_{1+x}\text{Te}_2$, *Journal of Solid State Chemistry* **53**, 415 (1984).
- [20] T. Ohtani, K. Hayashi, M. Nakahira, and H. Nozaki, Phase transition in $\text{V}_{1+x}\text{Te}_2$ ($0.04 < x < 0.11$), *Solid State Communications* **40**, 629 (1981).
- [21] A. A. Vinokurov, A. V. Tyurin, A. L. Emelina, K. S. Gavrichev, and V. P. Zlomanov, Thermodynamic properties of VTe_2 , *Inorganic Materials* **45**, 480 (2009).
- [22] C. W. Nicholson, M. Rumo, A. Pulkkinen, G. Kremer, B. Salzmänn, M.-L. Mottas, B. Hildebrand, T. Jaouen, T. K. Kim, S. Mukherjee, K. Ma, M. Muntwiler, F. O. von Rohr, C. Cacho, and C. Monney, Uniaxial strain-induced phase transition in the 2D topological semimetal IrTe_2 , *Communications Materials* **2**, 25 (2021).
- [23] N. Mitsuishi, Y. Sugita, M. S. Bahramy, M. Kamitani, T. Sonobe, M. Sakano, T. Shimojima, H. Takahashi, H. Sakai, K. Horiba, H. Kumigashira, K. Taguchi, K. Miyamoto, T. Okuda, S. Ishiwata, Y. Motome, and K. Ishizaka, Switching of band inversion and topological surface states by charge density wave, *Nature Communications* **11**, 2466 (2020).
- [24] C. Sohrt, A. Stange, M. Bauer, and K. Rossnagel, How fast can a peierls–mott insulator be melted?, *Faraday Discuss.* **171**, 243 (2014).
- [25] L. X. Yang, G. Rohde, K. Hanff, A. Stange, R. Xiong, J. Shi, M. Bauer, and K. Rossnagel, Bypassing the structural bottleneck in the ultrafast melting of electronic order, *Phys. Rev. Lett.* **125**, 266402 (2020).
- [26] F. Schmitt, P. S. Kirchmann, U. Bovensiepen, R. G. Moore, L. Rettig, M. Krenz, J.-H. Chu, N. Ru, L. Perfetti, D. H. Lu, M. Wolf, I. R. Fisher, and Z.-X. Shen, Transient Electronic Structure and Melting of a Charge Density Wave in TbTe_3 , *Science* **321**, 1649 (2008).
- [27] L. Rettig, R. Cortés, J.-H. Chu, I. R. Fisher, F. Schmitt, R. G. Moore, Z.-X. Shen, P. S. Kirchmann, M. Wolf, and

- U. Bovensiepen, Persistent order due to transiently enhanced nesting in an electronically excited charge density wave, *Nature Communications* **7**, 10459 (2016).
- [28] F. Schmitt, P. S. Kirchmann, U. Bovensiepen, R. G. Moore, J.-H. Chu, D. H. Lu, L. Rettig, M. Wolf, I. R. Fisher, and Z.-X. Shen, Ultrafast electron dynamics in the charge density wave material TbTe_3 , *New Journal of Physics* **13**, 063022 (2011).
- [29] J. Maklar, J. Sarkar, S. Dong, Y. A. Gerasimenko, T. Pincelli, S. Beaulieu, P. S. Kirchmann, J. A. Sobota, S. Yang, D. Leuenberger, R. G. Moore, Z.-X. Shen, M. Wolf, D. Mihailovic, R. Ernstorfer, and L. Rettig, Coherent light control of a metastable hidden state, *Science Advances* **9**, eadi4661 (2023).
- [30] M. Tuniz, D. Soranzio, D. Bidoggia, D. Puntel, W. Bronsch, S. L. Johnson, M. Peressi, F. Parmigiani, and F. Cilento, Ultrafast all-optical manipulation of the charge-density wave in VTe_2 , *Phys. Rev. Res.* **5**, 043276 (2023).
- [31] J. D. Budai, J. Hong, M. E. Manley, E. D. Specht, C. W. Li, J. Z. Tischler, D. L. Abernathy, A. H. Said, B. M. Leu, L. A. Boatner, R. J. McQueeney, and O. Delaire, Metallization of vanadium dioxide driven by large phonon entropy, *Nature* **515**, 535 (2014).
- [32] T. Huber, S. O. Mariager, A. Ferrer, H. Schäfer, J. A. Johnson, S. Gröbel, A. Lübcke, L. Huber, T. Kubacka, C. Dornes, C. Laulhe, S. Ravy, G. Ingold, P. Beaud, J. Demsar, and S. L. Johnson, Coherent structural dynamics of a prototypical charge-density-wave-to-metal transition, *Phys. Rev. Lett.* **113**, 026401 (2014).
- [33] A. D. Bruce, Structural phase transitions. ii. static critical behaviour, *Advances in Physics* **29**, 111 (1980).
- [34] A. M. Lindenberg, J. Larsson, K. Sokolowski-Tinten, K. J. Gaffney, C. Blome, O. Synnørgren, J. Sheppard, C. Caleman, A. G. MacPhee, D. Weinstein, D. P. Lowney, T. K. Allison, T. Matthews, R. W. Falcone, A. L. Cavalieri, D. M. Fritz, S. H. Lee, P. H. Bucksbaum, D. A. Reis, J. Rudati, P. H. Fuoss, C. C. Kao, D. P. Siddons, R. Pahl, J. Als-Nielsen, S. Duesterer, R. Ischebeck, H. Schlarb, H. Schulte-Schrepping, T. Tschentscher, J. Schneider, D. von der Linde, O. Hignette, F. Sette, H. N. Chapman, R. W. Lee, T. N. Hansen, S. Techert, J. S. Wark, M. Bergh, G. Huld, D. van der Spoel, N. Timneanu, J. Hajdu, R. A. Akre, E. Bong, P. Krejčík, J. Arthur, S. Brennan, K. Luening, and J. B. Hastings, Atomic-scale visualization of inertial dynamics, *Science* **308**, 392 (2005).
- [35] G. A. de la Peña Muñoz, A. A. Correa, S. Yang, O. Delaire, Y. Huang, A. S. Johnson, T. Katayama, V. Krapivin, E. Pastor, D. A. Reis, S. Teitelbaum, L. Vidas, S. Wall, and M. Trigo, Ultrafast lattice disordering can be accelerated by electronic collisional forces, *Nature Physics* **19**, 1489 (2023).
- [36] D. A. Keen and A. L. Goodwin, The crystallography of correlated disorder, *Nature* **521**, 303 (2015).
- [37] A. S. Johnson, E. Pastor, S. Batlle-Porro, H. Benzidi, T. Katayama, G. A. de la Peña Muñoz, V. Krapivin, S. Kim, N. López, M. Trigo, and S. E. Wall, All-optical seeding of a light-induced phase transition with correlated disorder, *Nature Physics* **20**, 970 (2024).
- [38] J. D. Rameau, S. Freutel, A. F. Kemper, M. A. Sentef, J. K. Freericks, I. Avigo, M. Ligges, L. Rettig, Y. Yoshida, H. Eisaki, J. Schneeloch, R. D. Zhong, Z. J. Xu, G. D. Gu, P. D. Johnson, and U. Bovensiepen, Energy dissipation from a correlated system driven out of equilibrium, *Nature Communications* **7**, 13761 (2016).
- [39] L. P. René de Cotret, J.-H. Pöhl, M. J. Stern, M. R. Otto, M. Sutton, and B. J. Siwick, Time- and momentum-resolved phonon population dynamics with ultrafast electron diffuse scattering, *Phys. Rev. B* **100**, 214115 (2019).
- [40] S. Girault, A. H. Moudden, and J. P. Pouget, Critical x-ray scattering at the peierls transition of the blue bronze, *Phys. Rev. B* **39**, 4430 (1989).
- [41] L. Perfetti, P. A. Loukakos, M. Lisowski, U. Bovensiepen, H. Eisaki, and M. Wolf, Ultrafast Electron Relaxation in Superconducting $\text{Bi}_2\text{Sr}_2\text{CaCu}_2\text{O}_{8+\delta}$ by Time-Resolved Photoelectron Spectroscopy, *Phys. Rev. Lett.* **99**, 197001 (2007).
- [42] L. Degiorgi, S. Thieme, B. Alavi, G. Grüner, R. H. McKenzie, K. Kim, and F. Levy, Fluctuation effects in quasi-one-dimensional conductors: Optical probing of thermal lattice fluctuations, *Phys. Rev. B* **52**, 5603 (1995).
- [43] R. H. McKenzie and J. W. Wilkins, Effect of lattice zero-point motion on electronic properties of the peierls-fröhlich state, *Phys. Rev. Lett.* **69**, 1085 (1992).
- [44] R. S. Kwok, G. Gruner, and S. E. Brown, Fluctuations and thermodynamics of the charge-density-wave phase transition, *Phys. Rev. Lett.* **65**, 365 (1990).
- [45] J. Maklar, M. Schüler, Y. W. Windsor, C. W. Nicholson, M. Puppín, P. Walmsley, I. R. Fisher, M. Wolf, R. Ernstorfer, M. A. Sentef, and L. Rettig, Coherent modulation of quasiparticle scattering rates in a photoexcited charge-density-wave system, *Phys. Rev. Lett.* **128**, 026406 (2022).
- [46] J. M. Harris, Z. X. Shen, P. J. White, D. S. Marshall, M. C. Schabel, J. N. Eckstein, and I. Bozovic, Anomalous superconducting state gap size versus T_c behavior in underdoped $\text{Bi}_2\text{Sr}_2\text{Ca}_{1-x}\text{Dy}_x\text{Cu}_2\text{O}_{8+\delta}$, *Phys. Rev. B* **54**, R15665 (1996).
- [47] H. Ding, T. Yokoya, J. C. Campuzano, T. Takahashi, M. Randeria, M. R. Norman, T. Mochiku, K. Kadowaki, and J. Giapintzakis, Spectroscopic evidence for a pseudogap in the normal state of underdoped high- T_c superconductors, *Nature* **382**, 51 (1996).
- [48] S. Cha, G. Lee, S. Lee, S. H. Ryu, Y. Sohn, G. An, C. Kang, M. Kim, K. Kim, A. Soon, and K. S. Kim, Order-disorder phase transition driven by interlayer sliding in lead iodides, *Nature Communications* **14**, 1981 (2023).
- [49] A. Picano, F. Grandi, and M. Eckstein, Inhomogeneous disordering at a photoinduced charge density wave transition, *Phys. Rev. B* **107**, 245112 (2023).
- [50] N. Erasmus, M. Eichberger, K. Haupt, I. Boshoff, G. Kassier, R. Birmurske, H. Berger, J. Demsar, and H. Schwoerer, Ultrafast Dynamics of Charge Density Waves in $4H_b$ -TaSe₂ Probed by Femtosecond Electron Diffraction, *Phys. Rev. Lett.* **109**, 167402 (2012).
- [51] A. Block, M. Liebel, R. Yu, M. Spector, Y. Sivan, F. J. G. de Abajo, and N. F. van Hulst, Tracking ultrafast hot-electron diffusion in space and time by ultrafast thermomodulation microscopy, *Science Advances* **5**, eaav8965 (2019).